Assisted Crystallization of Organometallic Cations by Interplay with Inorganic Anionic Clusters Units: Synthesis and Characterizations of the [Cp*(dppe)Fe–NCMe]$_2$·M_6L_{14} Series (M_6L_{14} = Cluster Unit: $[Re_6S_6Br_8]^{2-}$, $[Mo_6Br_{14}]^{2-}$ and $[Mo_6I_{14}]^{2-}$)

Guillaume Pilet,*[a–c] Kaplan Kirakci,[a] Frédéric de Montigny, Stéphane Cordier,[a] Claude Lapinte,[d] Christiane Perrin,[a] and André Perrin[a]

Keywords: Iron / Rhenium / Molybdenum octahedral clusters / M_6L_{14} units / Hybrid compounds / Inorganic organometallic chemistry / Single-crystal structures

Novel hybrid inorganic/organometallic compounds have been obtained from the crystallization of inorganic anionic clusters units with the [Cp*(dppe)Fe–NCMe]$^+$organometallic entity as the cationic counter part. After dissolution of $Cs_2M_6L_{14}$ (M_6L_{14} = $[Re_6S_6Br_8]^{2-}$, $[Mo_6Br_{14}]^{2-}$ and $[Mo_6I_{14}]^{2-}$) and [Cp*(dppe)Fe–NCMe]Cl precursors in acetonitrile at room temperature, the reaction proceeds by a metathesis of the Cl^- anion by $[M_6L_{14}]^{2-}$ anions and precipitation of CsCl. The crystal structures of the [Cp*(dppe)Fe–NCMe]$_2$[M_6L_{14}] series reveal that inorganic and organic entities can be assembled without any structural modifications to both partners whatever the M_6L_{14} unit. These properties of the M_6L_{14} cluster units could be extended for the crystallization of other novel organometallic cations when usual small counter anions do not lead to any crystallization with the new organometallic cation

Introduction

A wide variety of compounds based on M_6 clusters (M = Re, Mo) have been obtained by solid-state synthesis and extensively investigated.[1–5] Such compounds are built up from M_6L_{14} units (L = halogen, chalcogen) in which the M_6 cluster is face-capped by eight inner ligands (L^i) and six apical ligands (L^a) lie in terminal positions. The developed formula of the unit is then written as $M_6L^i{}_8L^a{}_6$ according to the H. Schäfer notation.[6] The condensation of units by means of apical-inner connections leads to solid-state compounds containing octahedral clusters with various physico-chemical properties such as superconductivity at high critical field,[7] catalytic[8] or redox intercalation behavior.[9] On the other hand, fascinating molecular and supramolecular assemblies based on axially substituted $M_6L^i{}_8$ cluster cores have been reported, particularly in rhenium cluster chemistry.[10] Their synthesis requires soluble cluster precursors with isolated $Re_6L^i{}_8L^a{}_6$ units. Numerous water-soluble cesium salts built up from isolated Re_6L_{14} units have been obtained from solid-state chemistry.[11] After dissolution in distilled water or acidic solutions, the $(TBA)_xRe_6L^i{}_8L^a{}_6$ series can be easily obtained by precipitation after addition of an excess of a TBA halide. The $(TBA)_xRe_6L^i{}_8L^a{}_6$ series, soluble in organic solvents, constitutes a set of relevant precursors for use in coordination chemistry.[1]

In this paper, we report the room-temperature synthesis and characterization of novel hybrid inorganic/organometallic compounds based on $[M_6L_{14}]^{2-}$ anionic units obtained by direct dissolution of $Cs_2M_6L_{14}$ in organic solvents ($[M_6L_{14}]^{2-}$ = $[Re_6S_6Br_8]^{2-}$, $[Mo_6Br_{14}]^{2-}$ and $[Mo_6I_{14}]^{2-}$). It will become evident that $[M_6L_{14}]^{2-}$ anionic units can be used to advantage in organometallic chemistry for the isolataton and characterization of new organometallic cations. Thus, the crystallization of large organometallic cations with small anions usually used in organometallic chemistry (for instance PF_6^-, BF_4^- or BPh_4^-), often affords single crystals with high mosaic spreads and low diffracting powers. Indeed, the quality of the single-crystal X-ray diffraction

[a] Institut de Chimie de Rennes, Laboratoire de Chimie du Solide et Inorganique Moléculaire, UMR 6511 CNRS – Université de Rennes 1,
Avenue du Général Leclerc, 35042 Rennes Cedex, France
[b] Arrhenius Laboratory, Department of Inorganic Chemistry, Stockholm University,
10691 Stockholm, Sweden
[c] Laboratoire des Multimatériaux et Interfaces, Université Claude Bernard Lyon 1, Bâtiment Berthollet,
43 Boulevard du 11 Novembre 1918, 69622 Villeurbanne Cedex, France
E-mail: guillaume@inorg.su.se
guillaume.pilet@univ-lyon1.fr
[d] Institut de Chimie de Rennes, Organométalliques et Catalyse: Chimie et Electrochimie Moléculaires, UMR 6509 CNRS – Université de Rennes 1,
Avenue du Général Leclerc, 35042 Rennes Cedex, France

 DOI: 10.1002/ejic.200400798

data often thwarts a structural solution or gives low reliability factors. The latter condition is the key point for obtaining accurate structural information on bond lengths and angles. In this work, we focused on the crystallization of the $[Cp^*(dppe)Fe–NCMe]^+$ organometallic cation with $[M_6L_{14}]^{2-}$ units ($[Re_6S_6Br_8]^{2-}$, $[Mo_6Br_{14}]^{2-}$ and $[Mo_6I_{14}]^{2-}$). The structures of the resultant $[Cp^*(dppe)Fe–NCMe]_2[M_6L_{14}]$ complexes, determined from single-crystal X-ray diffraction data, indicatee that inorganic and organic entities can be assembled without any structural modifications to both partners whatever the M_6L_{14} unit.

Single-Crystal X-ray Diffraction Analyses

Data Collection

Experimental details for $[Cp^*(dppe)FeNCCH_3]_2[Re_6(S_6Br_2)^iBr_6^a]$ (**1**), $[Cp^*(dppe)FeNCCH_3]_2[Mo_6Br_8{}^iBr_6^a]$ (**2**) and $[Cp^*(dppe)FeNCCH_3]_2[Mo_6I_8{}^iI_6^a]$ (**3**) are given in Table 1. Once the data processing had been performed by the KappaCCD analysis softwares,[12] the lattice constants were refined by least-squares refinements using 33851 reflections ($1.00° < \theta < 27.48°$), 10475 reflections ($2.55° < \theta < 27.48°$) and 14097 reflections ($2.72° < \theta < 30.03°$) for **1**, **2** and **3**, respectively. In each case, an absorption correction based on crystal shape was applied to the data sets with the ANALYTICAL program.[13]

Structure Solution and Refinement

The three compounds are isostructural and crystallize in the monoclinic system. According to the observed systematic extinctions, the structures were solved in the $P2_1/c$ space group (No. 14). The unit-cell parameters, crystal system, space group and refinement details are summarized in Table 1 for the three phases. The structures were solved by direct methods (SIR97 program[14]) combined with Fourier difference syntheses and refined against F using reflections with $I/\sigma(I) > 3$ (CRYSTALS program[15]).

In the case of the $[Cp^*(dppe)Fe–NCMe]_2[Re_6S_6Br_8]$ structure refinement, all ligand sites were at first considered as being occupied by bromine atoms. After several cycles of refinement, it turned out that only the inner sites were not fully occupied by bromine atoms. Sulfur atoms were then introduced to these inner sites with the same positions and the same atomic displacement parameters as those of the bromine atoms and for each crystallographic site the sum of the occupancies was restrained to the value corresponding to a fully occupied position. Afterwards, the two first constraints (on positional and atomic displacement parameters) were progressively relaxed during the convergence, leading to a final position in agreement with reliable Re–

Table 1. Crystallographic data[a] for $[Cp^*(dppe)Fe–NCCH_3]_2[Re_6S_6Br_8]$ (**1**), $[Cp^*(dppe)Fe–NCCH_3]_2[Mo_6Br_{14}]$ (**2**) and $[Cp^*(dppe)Fe–NCCH_3]_2[Mo_6I_{14}]$ (**3**).

	1	**2**	**3**
Refined formula	$Re_6S_{5.9(1)}S_{8.1(1)}Fe_2P_4N_2C_{76}$	$Mo_6Br_{14}Fe_2P_4N_2C_{76}$	$Mo_6I_{14}Fe_2P_4N_2C_{76}$
Formula mass (g mol^{-1})	3130.05	2870.80	3528.81
Crystallographic system	monoclinic	monoclinic	monoclinic
Unit-cell constants			
a [Å]	11.0059 (1)	10.9782 (1)	11.1154 (1)
b [Å]	24.0960 (3)	24.4768 (3)	25.3927 (2)
c [Å]	17.7444 (3)	17.6397 (2)	18.0104 (2)
β [°]	107.5597 (5)	107.1463 (8)	106.4890 (4)
V [Å^3]	4486.5 (1)	4529.32 (9)	4874.38 (8)
Space group	$P2_1/c$ (No. 14)	$P2_1/c$ (No. 14)	$P2_1/c$ (No. 14)
Z	2	2	2
T [K]	293	293	293
Density [g cm^{-3}]	2.32	2.10	2.40
μ [mm^{-1}]	122.29	73.98	55.70
θ range [°]	1.47; 27.48	2.55; 27.48	2.72; 30.03
Index range			
h	–14; 14	–14; 11	–15; 14
k	–30; 31	–31; 31	–35; 35
l	–23; 23	–21; 22	–25; 22
R[b]	0.0283	0.0362	0.0331
R_w[c]	0.0328	0.0422	0.0406
S	1.13	1.11	1.10
$\Delta\rho_{max}$ [e$^-$ Å^{-3}]	1.00	1.06	1.71
$\Delta\rho_{min}$ [e$^-$ Å^{-3}]	–1.12	–0.90	–1.22
No. of reflections used	4776	6617	8570
No. of parameters	514	470	470

[a] All data collected with Mo-K_α radiation (λ = 0.71069 Å). [b] $R = \Sigma(|F_o - F_c|)/\Sigma|F_o|$. [c] $R_w = \{\Sigma[w(|F_o - F_c|)^2]/\Sigma[w|F_o|^2]\}^{1/2}$.

Br and Re–S interatomic distances. Therefore, the chemical formula deduced from the X-ray diffraction refinement, $[Cp^*(dppe)Fe–NCMe]_2[(Re_6S^i_{5.9(1)}S^i_{2.1(1)})Br^a_6]$, is in good agreement with the EDS analyses.

All atoms of the cationic unit are located in 4*e* general crystallographic Wyckoff positions and were successfully refined anisotropically for the three structures (Figure 1). The refined formulae for **1**, **2** and **3** are given in Table 1. Atomic positions, equivalent thermal factors and occupancy factors are given in Table 2, Table 4 and Table 6. Meaningful bond lengths are summarized in Table 3, Table 5 and Table 7. All the thermal atomic displacements were refined anisotropically.

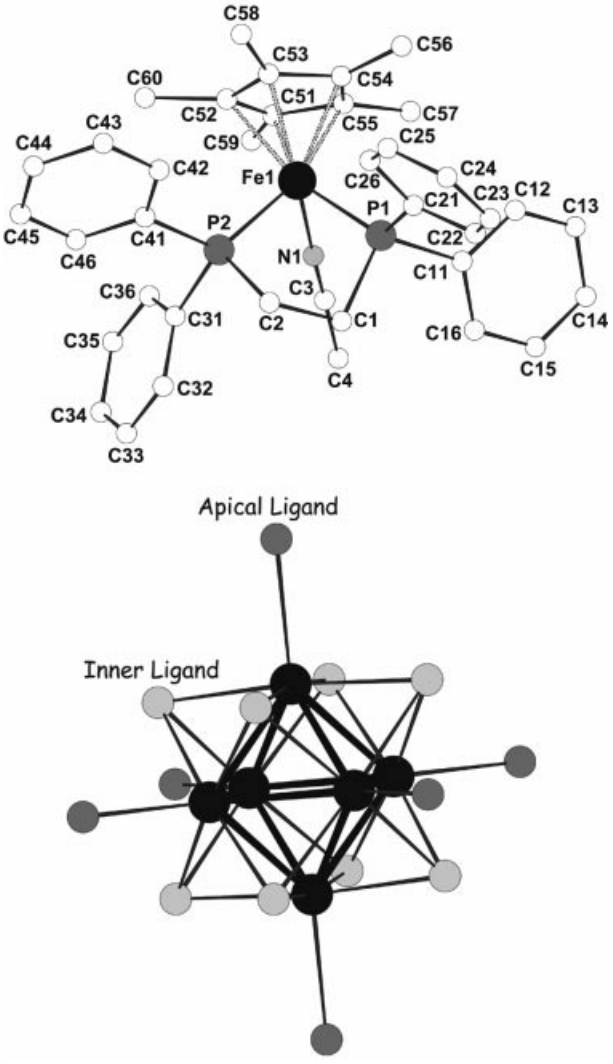

Figure 1. (a) Representation of the $[Cp^*(dppe)Fe–NCCH_3]^+$ cationic complex. The same labelling is used for the three structures. (b) Description of the $[Me_6L_{14}]$ (Me = Re, Mo; L = S, Br, I) anionic cluster entity.

Results

Structure of $[Cp^*(dppe)Fe–NCMe]_2[Re_6S_6Br_8]$

The structure of $[Cp^*(dppe)Fe–NCMe]_2[Re_6S_6Br_8]$ is based on a discrete $[Re_6S^i_6Br^i_2Br^a_6]^{2-}$ centrosymmetric cluster anion with an $(Re_6S^i_6Br^i_2)^{4+}$ cluster core. The Re_6 octahedron is slightly distorted and is inscribed into a cube of eight μ_3-S/Br atoms (inner ligands). Among the four independent inner ligand sites, all are randomly occupied by sulfur and bromine atoms [L^i1 = 0.39(1) S + 0.61(1) Br; L^i2 = 0.807(9) S + 0.193(9) Br; L^i3 = 0.903(8) S + 0.097(8) Br; L^i4 = 0.843(7) S + 0.157(7) Br]. The six apical positions are fully occupied by bromine atoms. The bond length ranges within the cluster unit are 2.5889(5)–2.6157(5) Å for Re–Re; 2.533(1)–2.5386(9) Å for Re–Br^a; 2.49(2)–2.66(5) Å for Re–Br^i and 2.403(7)–2.53(2) Å for Re–S^i (Table 3). These bond lengths correspond, within the s.u.'s, to those observed in the starting $Cs_2Re_6S_8Br_8$ cluster precursor. Indeed the substitution of $[Cp^*(dppe)Fe–NCMe]^+$ for Cs^+ does not influence the Re–Br^a bond length which is the most sensitive to a change in the counter cation in solid-state compounds.[16]

The bond lengths within the $[Cp^*(dppe)Fe–NCMe]^+$ cation in $[Cp^*(dppe)Fe–NCMe]_2[Re_6S_6Br_8]$ corresponds to those found in $[Cp^*(dppe)Fe–NCMe][PF_6]$.[17] The Fe^{II} atom is located in an environment built from a pentamethylcyclopentadienyl (Cp^*: $C_{10}H_{15}$), a P–$(CH_2)_2$–P bridge connected to four phenyl groups (dppe) and a molecule of acetonitrile (NCMe).

The Fe–C interatomic distances [2.097(9)–2.14(1) Å] and C–C bond lengths [1.41(2)–1.44(1) Å and 1.48(2)–1.55 (2) Å for C_5 ring and $C_5(CH_3)_5$, respectively] inside the Cp^* ligand are in good agreement with those generally observed for this kind of aromatic ring (average Fe–C distance equal to 2.11 Å, for example).[18–20]

Other selected interatomic distances are Fe–P [2.228(3)–2.258(3) Å], Fe–$NCCH_3$ [1.909(8) Å], P–C [1.833(9)–1.860(9) Å] and C–C [1.53(1) Å for the bridge, 1.34(2)–1.43(2) Å for aromatic rings inside the –P–$(CH_2)_2$–P– bridge], N–CCH_3 [1.15(1) Å] and NC–CH_3 [1.46(2) Å].

Structure of $[Cp^*(dppe)Fe–NCMe]_2[Mo_6Br_{14}]$

The anionic unit of the $[Cp^*(dppe)Fe–NCMe]_2[Mo_6Br_{14}]$ structure contains a slightly distorted Mo_6 octahedron. All the inner and apical positions of the cluster are occupied by bromine atoms. The chemical formula deduced from the X-ray diffraction refinement is $[Cp^*(dppe)Fe–NCMe]_2$-$[Mo_6Br_{14}]$ which fully corroborates with the EDS analysis. The ranges for the bond lengths within the cluster unit are 2.6358(6)–2.6437(6) Å for Mo–Mo, 2.5921(7)–2.6000(6) Å for Mo–Br^a and 2.5960(6)–2.6103(6) Å for Mo–Br^i (Table 5). Such values are comparable with data previously reported for the starting compound $Cs_2Mo_6Br_{14}$[23] (see Table 8). Indeed, the $[Cp^*(dppe)Fe–NCMe]^+$ cation does not influence the intra-unit bond lengths. The interatomic distances observed within the organometallic partner are very close to those observed in **1**.

Structure of $[Cp^*(dppe)Fe–NCMe]_2[Mo_6I_{14}]$

The structure of $[Cp^*(dppe)Fe–NCMe]_2[Mo_6I_{14}]$ is built from a slightly distorted Mo_6 octahedral cluster surrounded

Table 2. Atomic positions for $[Cp^*(dppe)Fe–NCCH_3]_2[Re_6S_6Br_8]$ (**1**).

Atom	Wyckoff position	*x*/*a*	*y*/*b*	*z*/*c*	$U(iso)_{eq.}$	Occ.
Re1	4*e*	0.41878(3)	0.54389(1)	0.91480(2)	0.0397	1
Re2	4*e*	0.52424(3)	0.44678(1)	0.93159(2)	0.0406	1
Re3	4*e*	0.65319(3)	0.53265(1)	0.00322(2)	0.0390	1
Br1	4*e*	0.3091(1)	0.60362(4)	0.79586(6)	0.0589	1
Br2	4*e*	0.5566(1)	0.37343(5)	0.83721(7)	0.0674	1
Br3	4*e*	0.86506(9)	0.57564(4)	0.00619(6)	0.0529	1
S1[a]	4*e*	0.252(2)	0.560(1)	0.975(1)	0.1009	0.39(1)
Br11[a]	4*e*	0.2425(3)	0.5646(2)	0.9820(3)	0.0470	0.61(1)
S2[a]	4*e*	0.5420(7)	0.6223(3)	0.9859(5)	0.0439	0.807(9)
Br21[a]	4*e*	0.545(2)	0.6264(5)	0.991(1)	0.0774	0.193(9)
S3[a]	4*e*	0.3051(6)	0.4609(2)	0.8560(7)	0.0447	0.903(8)
Br31[a]	4*e*	0.297(3)	0.460(1)	0.841(3)	0.0679	0.097(8)
S4[a]	4*e*	0.5882(7)	0.5215(3)	0.8606(4)	0.0565	0.843(7)
Br41[a]	4*e*	0.595(2)	0.5221(4)	0.8538(8)	0.0521	0.157(7)
Fe1	4*e*	–0.1005(1)	0.31715(5)	0.58432(7)	0.0421	1
P1	4*e*	0.0904(2)	0.32193(9)	0.5655(1)	0.0420	1
P2	4*e*	–0.0989(2)	0.41082(9)	0.5824(1)	0.0451	1
C1	4*e*	0.1539(9)	0.3919(4)	0.6001(6)	0.0504	1
C2	4*e*	0.0480(9)	0.4330(4)	0.5596(6)	0.0536	1
N1	4*e*	–0.0035(7)	0.3187(3)	0.6934(5)	0.0467	1
C3	4*e*	0.055(1)	0.3180(4)	0.7588(6)	0.0539	1
C4	4*e*	0.133(2)	0.3194(6)	0.8413(7)	0.0919	1
C30	4*e*	0.2138(8)	0.2743(4)	0.6225(5)	0.0453	1
C31	4*e*	0.2144(9)	0.2186(4)	0.5980(6)	0.0553	1
C32	4*e*	0.3014(9)	0.1808(4)	0.6418(7)	0.0611	1
C33	4*e*	0.395(1)	0.1982(4)	0.7106(7)	0.0661	1
C34	4*e*	0.397(1)	0.2527(5)	0.7334(7)	0.0750	1
C35	4*e*	0.3087(9)	0.2904(4)	0.6903(6)	0.0596	1
C40	4*e*	0.1167(8)	0.3232(4)	0.4684(5)	0.0479	1
C41	4*e*	0.237(1)	0.3146(5)	0.4610(6)	0.0672	1
C42	4*e*	0.256(1)	0.3264(7)	0.3887(8)	0.0913	1
C43	4*e*	0.161(1)	0.3456(7)	0.3242(7)	0.0884	1
C44	4*e*	0.042(1)	0.3521(6)	0.3314(7)	0.0825	1
C45	4*e*	0.015(1)	0.3401(5)	0.4036(5)	0.0586	1
C50	4*e*	–0.0867(9)	0.4430(4)	0.6777(5)	0.0488	1
C51	4*e*	–0.009(1)	0.4891(5)	0.7071(6)	0.0629	1
C52	4*e*	–0.009(1)	0.5129(6)	0.7800(7)	0.0806	1
C53	4*e*	–0.084(1)	0.4933(6)	0.8206(7)	0.0776	1
C54	4*e*	–0.163(1)	0.4465(5)	0.7929(8)	0.0812	1
C55	4*e*	–0.162(1)	0.4228(5)	0.7225(7)	0.0720	1
C60	4*e*	–0.2196(9)	0.4544(4)	0.5135(6)	0.0524	1
C61	4*e*	–0.246(1)	0.4458(4)	0.4335(6)	0.0618	1
C62	4*e*	–0.339(1)	0.4789(5)	0.3776(7)	0.0718	1
C63	4*e*	–0.403(1)	0.5203(5)	0.4067(9)	0.0789	1
C64	4*e*	–0.374(1)	0.5292(5)	0.4866(8)	0.0730	1
C65	4*e*	–0.2826(9)	0.4962(4)	0.5407(7)	0.0641	1
C70	4*e*	–0.235(1)	0.2674(4)	0.6176(7)	0.0610	1
C71	4*e*	–0.2992(9)	0.3050(5)	0.5577(8)	0.0677	1
C72	4*e*	–0.262(1)	0.2932(5)	0.4886(7)	0.0709	1
C73	4*e*	–0.1725(9)	0.2488(4)	0.5068(6)	0.0543	1
C74	4*e*	–0.1540(8)	0.2339(4)	0.5880(6)	0.0494	1
C80	4*e*	–0.250(1)	0.2629(5)	0.6989(8)	0.0812	1
C81	4*e*	–0.406(1)	0.3452(6)	0.562(1)	0.0984	1
C82	4*e*	–0.329(1)	0.3136(6)	0.4044(8)	0.1026	1
C83	4*e*	–0.123(1)	0.2187(5)	0.4500(6)	0.0687	1
C84	4*e*	–0.070(1)	0.1869(5)	0.6298(7)	0.0705	1

[a] For inner ligands, these atoms correspond to a split position.

by eight inner iodine ligands and six apical iodine ligands. As expected, owing to the larger ionic radius of iodine face-capping ligands compared with bromine, the Mo–Mo bonds are longer in $[Cp^*(dppe)Fe–NCMe]_2[Mo_6I_{14}]$ than in $[Cp^*(dppe)Fe–NCMe]_2[Mo_6Br_{14}]$. The chemical formula deduced from the X-ray diffraction refinement is $[Cp^*(dppe)Fe–NCMe]_2[Mo_6I_{14}]$ which is fully consistent with the EDS analysis. The bond length ranges within the

Table 3. Selected interatomic distances [Å] for $[Cp^*(dppe)Fe–NCCH_3]_2[Re_6S_6Br_8]$ (**1**).

Anionic unit: $[Re_6(S_6Br_2)^iBr^a_8]^{2-}$					
Re–Re bond lengths					
Re1–Re2	2.5890(5)	Re1–Re3	2.5979(5)	Re1–Re3	2.6154(5)
Re1–Re2	2.6157(5)	Re2–Re3	2.6000(5)	Re2–Re3	2.6118(5)
$Re–Br^a$ bond lengths (^{a}: apical ligand)					
Re1–Br1	2.5386(9)	Re2–Br2	2.533(1)	Re3–Br3	2.538(1)
$Re–Br^i$ bond lengths (^{i}: inner ligand)					
Re1–Br11	2.613(5)	Re1–Br21	2.56(1)	Re1–Br31	2.56(2)
Re1–Br41	2.54(1)	Re2–Br11	2.577(3)	Re2–Br21	2.49(2)
Re2–Br31	2.55(2)	Re2–Br41	2.54(1)	Re3–Br11	2.587(5)
Re3–Br21	2.53(1)	Re3–Br31	2.66(5)	Re3–Br41	2.55(1)
$Re–S^i$ bond lengths (^{i}: inner ligand)					
Re1–S1	2.42(2)	Re1–S2	2.442(7)	Re1–S3	2.422(5)
Re1–S4	2.403(7)	Re2–S1	2.53(2)	Re2–S2	2.467(7)
Re2–S3	2.404(5)	Re2–S4	2.421(7)	Re3–S1	2.45(2)
Re3–S2	2.455(7)	Re3–S3	2.41(1)	Re3–S4	2.428(7)
Cationic unit: $[Cp^*(dppe)Fe–NCCH_3]^+$					
Fe–X distances and bond lengths					
X = Cp*					
Fe1–C70	2.13(1)	Fe1–C71	2.11(1)	Fe1–C72	2.14(1)
Fe1–C73	2.138(9)	Fe1–C74	2.097(9)		
X = (dppe)					
Fe1–P1	2.228(3)	Fe1–P2	2.258(3)		
$X = NCCH_3$					
Fe1–N1	1.909(8)				
Cp* intra-bond lengths					
C70–C71	1.41(3)	C71–C72	1.43(2)	C72–C73	1.43(2)
C73–C74	1.44(1)	C74–C70	1.42(1)		
C70–C80	1.50(2)	C71–C81	1.55(2)	C72–C82	1.53(2)
C73–C83	1.48(2)	C74–C84	1.51(1)		
(dppe) intra-bond lengths					
P1–C1	1.857(9)	C1–C2	1.53(1)	C2–P2	1.860(9)
P1–C30	1.833(9)	P1–C40	1.831(9)	P2–C50	1.83(1)
P2–C60	1.839(9)				
C30–C31	1.41(1)	C31–C32	1.38(1)	C32–C33	1.40(1)
C33–C34	1.37(2)	C34–C35	1.38(1)	C35–C30	1.39(1)
C40–C41	1.39(1)	C41–C42	1.39(2)	C42–C43	1.38(2)
C43–C42	1.38(2)	C44–C45	1.43(2)	C45–C40	1.40(1)
C50–C51	1.40(1)	C51–C52	1.41(2)	C52–C53	1.34(2)
C53–C54	1.41(2)	C54–C55	1.38(2)	C55–C50	1.39(2)
C60–C61	1.38(1)	C61–C62	1.43(1)	C62–C63	1.40(2)
C63–C64	1.37(2)	C64–C65	1.41(1)	C65–C60	1.39(1)
$–NCCH_3$ intra-bond lengths					
N1–C3	1.15(1)	C3–C4	1.46(2)		

anionic unit are 2.6745(5)–2.6878(6) Å for Mo–Mo, 2.8408(5)–2.8467(5) Å for $Mo–I^a$ and 2.7665(5)–2.7889(5) Å for $Mo–I^i$ (Table 7). These distances are in good agreement with those found in the starting compound $Cs_2Mo_6I_{14}$[23] (see Table 8). The interatomic distances within the organometallic cation are identical to the values observed in **1** and **2**.

General Description of the Three Structures

The structures of the three original compounds are based on discrete $[M_6L_{14}]^{2-}$ anions (M = Mo, Re; L = Br, I, S) located at the corners and the centre of two opposite faces of the unit-cell (Figure 2), thus forming a pseudo-*A*-centered monoclinic unit-cell. Owing to the symmetry of the cationic $[Cp^*(dppe)Fe–NCMe]^+$ group, the space group is $P2_1/n$ and the systematic extinctions corresponding to the *A* lattice are not observed. The structural cohesion results from coulombic interactions between anionic inorganic units and cationic entities based on organo–iron molecules.

The structures of the compounds in the $[Cp^*(dppe)Fe–NCMe]_2{\cdot}M_6L_{14}$ series can be described in each case as a succession of $[M_6L_{14}]^{2-}$ anionic units layers and cationic layers. The layers of anionic entities are planar whilst the layers of $[Cp^*(dppe)Fe–NCMe]^+$ cations are puckered along the *a* axis of the unit-cell (Figure 3). The shortest Fe–Fe distances between two consecutive cationic planes are equal to 11.01, 10.98 and 11.12 Å for $[Cp^*(dppe)Fe–NCMe]_2[Re_6S_6Br_8]$, $[Cp^*(dppe)Fe–NCMe]_2[Mo_6Br_{14}]$ and $[Cp^*(dppe)Fe–NCMe]_2[Mo_6I_{14}]$, respectively. The shortest Fe–Fe distances within the puckered plane of cations are 9.44, 9.83 and 9.74 Å for these three compounds, respectively. For comparison, the Fe–Fe distance in $[Cp^*(dppe)Fe–NCMe][PF_6]$ is 9.099 Å.

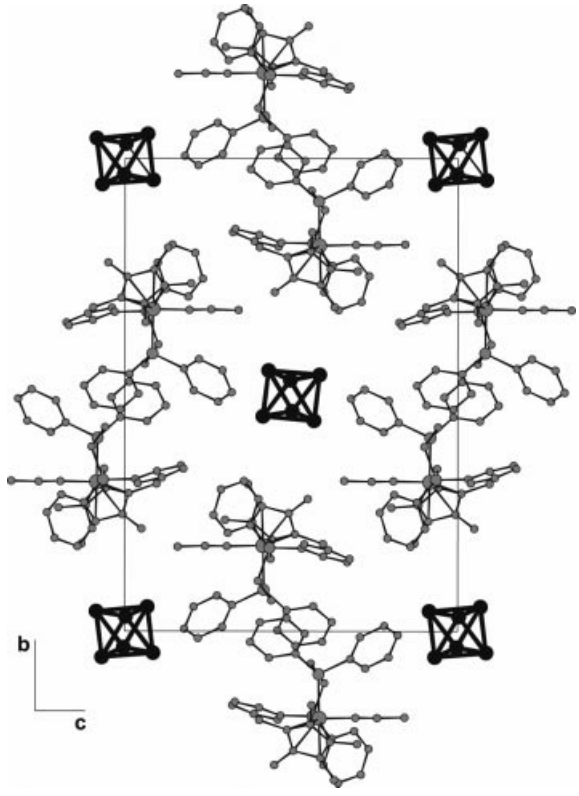

Figure 2. $[Cp^*(dppe)Fe–NCCH_3]_2[Me_6L_{14}]$ (Me = Re, Mo; L = S, Br, I) structure projection in the (*b*,*c*) plane of the unit-cell. For clarity, cluster ligands have been removed.

Table 4. Atomic positions for $[Cp^*(dppe)Fe–NCCH_3]_2[Mo_6Br_{14}]$ (**2**).

Atom	Wyckoff position	*x/a*	*y/b*	*z/c*	$U(iso)_{equiv.}$	Occ.
Mo1	4*e*	0.47207(4)	0.05236(2)	0.06998(2)	0.0341	1
Mo2	4*e*	0.34605(4)	–0.03384(2)	–0.00290(2)	0.0334	1
Mo3	4*e*	0.58474(4)	–0.04383(2)	0.08587(2)	0.0339	1
Br1	4*e*	0.23650(5)	0.06150(2)	–0.01869(3)	0.0409	1
Br2	4*e*	0.40469(5)	–0.02484(2)	0.15091(3)	0.0403	1
Br3	4*e*	0.53910(5)	0.12851(2)	–0.01209(3)	0.0427	1
Br4	4*e*	0.70768(5)	0.04185(2)	0.15669(3)	0.0418	1
Br5	4*e*	0.13158(5)	–0.07986(2)	–0.00518(3)	0.0470	1
Br6	4*e*	0.69729(6)	–0.10414(2)	0.20771(3)	0.0510	1
Br7	4*e*	0.43641(6)	0.12481(2)	0.16849(4)	0.0585	1
Fe1	4*e*	0.10199(6)	0.18095(3)	0.41408(4)	0.0355	1
P1	4*e*	0.0984(1)	0.08889(5)	0.41616(8)	0.0393	1
P2	4*e*	–0.0893(1)	0.17715(5)	0.43394(7)	0.0364	1
C1	4*e*	–0.0495(5)	0.0677(2)	0.4388(4)	0.0461	1
C2	4*e*	–0.1517(5)	0.1090(2)	0.3992(3)	0.0448	1
N1	4*e*	0.0039(4)	0.1811(2)	0.3053(2)	0.0398	1
C3	4*e*	–0.0562(6)	0.1834(2)	0.2405(3)	0.0480	1
C4	4*e*	–0.1321(8)	0.1854(3)	0.1580(4)	0.0769	1
C30	4*e*	0.2185(5)	0.0458(2)	0.4848(3)	0.0425	1
C31	4*e*	0.2836(6)	0.0047(3)	0.4586(4)	0.0549	1
C32	4*e*	0.3740(6)	–0.0276(3)	0.5126(4)	0.0628	1
C33	4*e*	0.3996(6)	–0.0195(3)	0.5921(5)	0.0641	1
C34	4*e*	0.3333(7)	0.0204(3)	0.6204(4)	0.0653	1
C35	4*e*	0.2421(6)	0.0525(3)	0.5663(4)	0.0560	1
C40	4*e*	0.0838(5)	0.0557(2)	0.3205(3)	0.0426	1
C41	4*e*	0.0166(6)	0.0074(3)	0.2968(4)	0.0564	1
C42	4*e*	0.0150(7)	–0.0173(3)	0.2251(4)	0.0615	1
C43	4*e*	0.0786(7)	0.0067(3)	0.1767(4)	0.0639	1
C44	4*e*	0.1452(7)	0.0538(3)	0.1983(4)	0.0639	1
C45	4*e*	0.1492(6)	0.0786(3)	0.2716(4)	0.0548	1
C50	4*e*	–0.2125(5)	0.2239(2)	0.3776(3)	0.0406	1
C51	4*e*	–0.2085(5)	0.2788(2)	0.4009(3)	0.0484	1
C52	4*e*	–0.2972(6)	0.3157(3)	0.3578(4)	0.0562	1
C53	4*e*	–0.3931(6)	0.2999(3)	0.2923(4)	0.0610	1
C54	4*e*	–0.3991(6)	0.2455(3)	0.2687(4)	0.0637	1
C55	4*e*	–0.3096(6)	0.2075(2)	0.3112(3)	0.0511	1
C60	4*e*	–0.1168(5)	0.1760(2)	0.5309(3)	0.0458	1
C61	4*e*	–0.2383(6)	0.1839(3)	0.5383(4)	0.0619	1
C62	4*e*	–0.2582(7)	0.1745(4)	0.6127(4)	0.0768	1
C63	4*e*	–0.1613(8)	0.1558(4)	0.6767(4)	0.0790	1
C64	4*e*	–0.0407(7)	0.1495(3)	0.6697(4)	0.0646	1
C65	4*e*	–0.0184(6)	0.1591(3)	0.5969(3)	0.0502	1
C70	4*e*	0.1586(5)	0.2633(2)	0.4125(3)	0.0442	1
C71	4*e*	0.1792(6)	0.2466(2)	0.4926(3)	0.0489	1
C72	4*e*	0.2651(6)	0.2028(3)	0.5079(4)	0.0564	1
C73	4*e*	0.3011(5)	0.1917(3)	0.4373(4)	0.0553	1
C74	4*e*	0.2360(6)	0.2289(2)	0.3796(4)	0.0510	1
C80	4*e*	0.0782(7)	0.3102(3)	0.3717(4)	0.0625	1
C81	4*e*	0.1321(7)	0.2768(3)	0.5536(4)	0.0690	1
C82	4*e*	0.3372(7)	0.1819(3)	0.5919(5)	0.0822	1
C83	4*e*	0.4043(6)	0.1529(3)	0.4305(6)	0.0825	1
C84	4*e*	0.2507(8)	0.2369(3)	0.2974(5)	0.0711	1

Discussion and Conclusion

The crystal structures of the $[Cp^*(dppe)Fe–NCMe]_2 \cdot M_6L_{14}$ series reveal that inorganic and organic entities can be assembled without any structural modifications to each-partner whatever the M_6L_{14} unit (Table 8). Indeed, the interatomic distances within the M_6L_{14} units do not significantly vary between the starting $Cs_2M_6L_{14}$ solid-state compound and the final $[Cp^*(dppe)Fe–NCMe]_2 \cdot M_6L_{14}$ series. Furthermore, the interatomic distances within the $[Cp^*(dppe)Fe–NCMe]^+$ entity correspond to those found in the previously reported $[Cp^*(dppe)Fe–NCMe][PF_6]$. The compound $[Cp^*(dppe)Fe–NCMe]PF_6$ was obtained by photolysis of $[Cp^*Fe–(CO)_3]PF_6$ in acetonitrile with 1 equiv. of dppe. After the reaction, single crystals were ob-

Table 5. Selected inter-atomic distances [Å] for $[Cp^*(dppe)Fe–NCCH_3]_2[Mo_6Br_{14}]$ (**2**).

Anionic unit: $[Mo_6Br^i_8Br^a_6]^{2-}$					
Mo–Mo bond lengths					
Mo1–Mo2	2.6402(5)	Mo1–Mo2	2.6429(6)	Mo1–Mo3	2.6358(6)
Mo1–Mo3	2.6419(5)	Mo2–Mo3	2.6379(5)	Mo2–Mo3	2.6437(6)
$Mo–Br^a$ bond lengths (^{a}: apical ligand)					
Mo1–Br7	2.5921(7)	Mo2–Br5	2.5996(7)	Mo3–Br6	2.6000(6)
$Mo–Br^i$ bond lengths (^{i}: inner ligand)					
Mo1–Br1	2.6076(6)	Mo1–Br2	2.6037(6)	Mo1–Br3	2.5960(6)
Mo1–Br4	2.6007(6)	Mo2–Br1	2.6024(6)	Mo2–Br2	2.6067(6)
Mo2–Br3	2.6139(6)	Mo2–Br4	2.6081(6)	Mo3–Br1	2.6103(6)
Mo3–Br2	2.6031(6)	Mo3–Br3	2.6068(6)	Mo3–Br4	2.6050(6)
Cationic unit: $[Cp^*(dppe)Fe–NCCH_3]^+$					
Fe–X distances and bond lengths					
X = Cp*					
Fe1–C70	2.112(5)	Fe1–C71	2.128(5)	Fe1–C72	2.118(6)
Fe1–C73	2.118(6)	Fe1–C74	2.108(5)		
X = (dppe)					
Fe1–P1	2.254(2)	Fe1–P2	2.231(1)		
X = $NCCH_3$					
Fe1–N1	1.903(4)				
Cp* intra-bond lengths					
C70–C71	1.422(8)	C71–C72	1.400(9)	C72–C73	1.44(1)
C73–C74	1.396(9)	C74–C70	1.435(8)		
C70–C80	1.497(9)	C71–C81	1.516(9)	C72–C82	1.547(9)
C73–C83	1.51(1)	C74–C84	1.517(9)		
(dppe) intra-bond lengths					
P1–C1	1.858(5)	C1–C2	1.520(8)	C2–P2	1.838(5)
P1–C30	1.837(5)	P1–C40	1.836(5)	P2–C50	1.826(5)
P2–C60	1.822(5)				
C30–C31	1.390(8)	C31–C32	1.399(9)	C32–C33	1.36(1)
C33–C34	1.40(1)	C34–C35	1.402(9)	C35–C30	1.393(9)
C40–C41	1.393(8)	C41–C42	1.396(9)	C42–C43	1.38(1)
C43–C44	1.36(1)	C44–C45	1.418(9)	C45–C40	1.391(8)
C50–C51	1.401(8)	C51–C52	1.381(8)	C52–C53	1.370(9)
C53–C54	1.390(9)	C54–C55	1.400(8)	C55–C50	1.390(7)
C60–C61	1.392(8)	C61–C62	1.411(9)	C62–C63	1.38(1)
C63–C64	1.37(1)	C64–C65	1.397(9)	C65–C60	1.398(8)
$–NCCH_3$ intra-bond lengths					
N1–C3	1.141(7)	C3–C4	1.449(8)		

tained by slowly cooling the solution to 233K. This procedure cannot guarantee a rigorous control of the crystallization and cannot be extended to brittle entities or those unstable at lowtemperatures. On the other hand, [Cp*(dppe)Fe–NCMe] is easily crystallized at room temperature with M_6L_{14} units. The reaction proposed here for the synthesis of the $[Cp^*(dppe)Fe–NCMe]_2 \cdot M_6L_{14}$ series is based on the exchange, in solution, of the chlorine atom from the Cp*(dppe)FeCl precursor by the more strongly coordinating acetonitrile group.[21] The charge is then compensated for by the M_6L_{14} dianionic unit. Using an organic solvent, it is more easy to separate CsCl than TBACl from $[Cp^*(dppe)Fe–NCMe]_2[Mo_6L_{14}]$. TBACl results from the reaction between [Cp*(dppe)Fe–NCMe]Cl and $(TBA)_2$-Mo_6L_{14} indicating that $Cs_2Mo_6L_{14}$ solid-state compounds must be preferentially chosen instead of the $(TBA)_2Mo_6L_{14}$ series usually used in coordination chemistry. M_6L_{14} anionic units could be used for the crystallization of other novel cationic organometallic entities when usual anionic counterparts give unfruitful results. In particular, the $Cs_2M_6L_{14}$ series could be used to advantage instead of $MReX_6$ salts for the crystallization of organic or organometallic cations from chloride precursors by precipitation of CsCl.

Finally, it is noteworthy that a solubile cation needs to counterbalance an insolubile anion to favour the crystal growing process.

Experimental Section

General: Unless otherwise specified, all reagents and solvents were purchased from commercial suppliers and used without further purification. The complex (η^2-dppe)(η^5-C_5Me_5)FeCl was prepared as described.[21][1]H NMR spectra were recorded with a Bruker Avance 200 (200 MHz) spectrometer. ^1H and ^{31}P NMR chemical shifts are reported in units of parts per million relative to the residual protio solvent and H_3PO_4, respectively.Transmittance-FTIR spectra were recorded with a Bruker IFS28 spectrometer (400–4000 cm^{-1}). $Cs_2Re_6S_6Br_8$, as well as $Cs_2Mo_6Br_{14}$ and $Cs_2Mo_6I_{14}$ were prepared by solid-state reactions as described in refs.[22,23], respectively. Chemical analyses were performed by energy dispersive spectrometry (EDS), using a scanning electron microscope JEOL JSM 6400 equipped with a microprobe EDS Oxford Link ISIS. Single-crystal X-ray diffraction data collections were performed at room temperature with a Nonius KappaCCD diffractometer. CCDC-244494, -250568 {for $[Cp^*(dppe)Fe–NCMe]_2[Re_6S_6Br_8]$, $[Cp^*(dppe)Fe–NCMe]_2[Mo_6Br_{14}]$} and CCDC-250569 {for $[Cp^*(dppe)Fe–NCMe]_2[Mo_6I_{14}]$} contain the supplementary crystallographic data for this paper. These data can be obtained free of charge from The Cambridge Crystallographic Data Centre via www.ccdc.cam.ac.uk/data_request/cif.

Synthesis of $[Cp^*(dppe)Fe–NCMe]_2[Re_6S_6Br_8]$ (1): [Cp*(dppe)FeCl] (0.312 g; 0.5 mmol) and $Cs_2Re_6S_6Br_8$ (0.609 g; 0.25 mmol) were separately dissolved in degassed MeCN (10 mL and 50 mL, respectively) in Schlenk tubes. The solutions were then mixed together with magnetic stirring for 1 h. The solvent was subsequently removed. $[Cp^*(dppe)Fe–NCMe]_2[Re_6S_6Br_8]$ was extracted from the resultant product by addition of acetone. The orange solution was then separated from the CsCl precipitate by filtration. After evaporation of acetone, $[Cp^*(dppe)Fe–NCMe]_2[Re_6S_6Br_8]$ was obtained as a brown powder (yield 40 %). Single crystals suitable for X-ray diffraction studies were obtained by diffusion of pentane into an acetone solution. No traces of chlorine or cesium were apparent in the final product from the EDS analysis (experimental atomic percentages: Fe, P, Re, S, Br: 7.0, 17.3, 24.1, 23.8, 27.8; calculated for $[Cp^*(dppe)Fe–CMe]_2[Re_6S_6Br_8]$: 7.7, 15.4, 23.1, 23.1, 30.8). This result is consistent with a complete cationic exchange between $[Re_6S_6Br_8]$ dianionic units and Cl^- with precipitation of CsCl in an organic solvent. In agreement with previous data reported with the related PF_6 salt,[24] the ^{31}P NMR spectrum exhibits only one signal at δ = 91.13 ppm characteristic for the two P atoms of the –P–$(CH_2)_2$–P– chain bridging the central iron atom. The presence of a

Table 6. Atomic positions for $[Cp^*(dppe)Fe–NCCH_3]_2[Mo_6I_{14}]$ (**3**).

Atom	Wyckoff position	*x*/*a*	y/*b*	*z*/*c*	$U(iso)_{equiv.}$	Occ.
Mo1	4*e*	–0.97087(4)	0.54948(2)	0.42827(2)	0.0296	1
Mo2	4*e*	–1.08147(4)	0.45503(2)	0.41714(2)	0.0293	1
Mo3	4*e*	–0.84480(3)	0.46681(2)	0.50508(2)	0.0288	1
I1	4*e*	–0.72438(3)	0.56333(1)	0.51756(2)	0.0377	1
I2	4*e*	–1.21536(3)	0.53925(1)	0.33469(2)	0.0383	1
I3	4*e*	–0.89424(3)	0.47067(1)	0.34503(2)	0.0369	1
I4	4*e*	–1.19610(4)	0.38744(2)	0.29125(2)	0.0479	1
I5	4*e*	–1.04416(3)	0.63242(1)	0.50508(2)	0.0386	1
I6	4*e*	–0.61208(3)	0.41816(2)	0.50963(2)	0.0440	1
I7	4*e*	–0.92918(4)	0.62303(2)	0.31917(3)	0.0543	1
Fe1	4*e*	–0.39819(7)	0.17697(3)	0.41956(5)	0.0371	1
P1	4*e*	–0.4039(1)	0.08851(6)	0.42454(9)	0.0401	1
P2	4*e*	–0.5869(1)	0.17556(6)	0.44063(8)	0.0390	1
N1	4*e*	–0.4940(5)	0.1770(2)	0.3137(3)	0.0440	1
C1	4*e*	–0.5486(6)	0.0707(2)	0.4493(4)	0.0474	1
C2	4*e*	–0.6514(5)	0.1096(2)	0.4092(4)	0.0448	1
C3	4*e*	–0.5522(7)	0.1808(3)	0.2498(4)	0.0534	1
C4	4*e*	–0.623(1)	0.1856(4)	0.1687(4)	0.0879	1
C30	4*e*	–0.2856(6)	0.0467(3)	0.4918(4)	0.0465	1
C31	4*e*	–0.2671(7)	0.0526(3)	0.5716(4)	0.0569	1
C32	4*e*	–0.1774(9)	0.0210(3)	0.6230(5)	0.0700	1
C33	4*e*	–0.1098(7)	–0.0167(3)	0.5960(6)	0.0727	1
C34	4*e*	–0.1301(7)	–0.0222(3)	0.5168(5)	0.0670	1
C35	4*e*	–0.2172(6)	0.0099(3)	0.4651(4)	0.0571	1
C40	4*e*	–0.4190(5)	0.0539(2)	0.3326(3)	0.0423	1
C41	4*e*	–0.4790(7)	0.0058(3)	0.3152(4)	0.0547	1
C42	4*e*	–0.4821(7)	–0.0209(3)	0.2475(5)	0.0633	1
C43	4*e*	–0.4259(6)	0.0011(3)	0.1945(5)	0.0597	1
C44	4*e*	–0.3662(7)	0.0495(3)	0.2112(5)	0.0616	1
C45	4*e*	–0.3612(6)	0.0759(3)	0.2799(4)	0.0512	1
C50	4*e*	–0.6137(5)	0.1776(3)	0.5360(4)	0.0453	1
C51	4*e*	–0.5198(6)	0.1638(3)	0.6015(4)	0.0513	1
C52	4*e*	–0.5418(8)	0.1577(4)	0.6735(4)	0.0679	1
C53	4*e*	–0.6625(9)	0.1657(4)	0.6799(5)	0.0793	1
C54	4*e*	–0.7577(8)	0.1804(5)	0.6146(5)	0.0853	1
C55	4*e*	–0.7349(7)	0.1862(4)	0.5434(4)	0.0638	1
C60	4*e*	–0.7057(5)	0.2210(2)	0.3848(3)	0.0417	1
C61	4*e*	–0.7017(6)	0.2736(3)	0.4071(4)	0.0523	1
C62	4*e*	–0.7868(7)	0.3103(3)	0.3636(5)	0.0601	1
C63	4*e*	–0.8786(7)	0.2951(3)	0.2978(5)	0.0603	1
C64	4*e*	–0.8839(8)	0.2424(3)	0.2758(5)	0.0725	1
C65	4*e*	–0.7989(7)	0.2051(3)	0.3186(4)	0.0575	1
C70	4*e*	–0.2361(6)	0.1977(3)	0.5103(4)	0.0540	1
C71	4*e*	–0.2016(6)	0.1858(3)	0.4410(5)	0.0553	1
C72	4*e*	–0.3417(6)	0.2560(2)	0.4164(4)	0.0488	1
C73	4*e*	–0.2647(6)	0.2221(2)	0.3834(4)	0.0506	1
C74	4*e*	–0.3205(6)	0.2410(3)	0.4947(4)	0.0488	1
C80	4*e*	–0.1710(9)	0.1779(4)	0.5919(6)	0.0894	1
C81	4*e*	–0.0996(7)	0.1477(4)	0.4343(7)	0.0859	1
C82	4*e*	–0.2497(9)	0.2283(3)	0.3034(5)	0.0716	1
C83	4*e*	–0.4184(7)	0.3005(3)	0.3748(5)	0.0614	1
C84	4*e*	–0.3648(8)	0.2715(3)	0.5531(5)	0.0678	1

unique singlet is evidence the formation of only one organometallic complex with an η^2-dppe ligand. The ^{1}H NMR spectrum exhibits several peaks, i.e. a group between δ = 7.34 and 7.70 ppm (20 hydrogen atoms of the four phenyl groups connected to the two P atoms), a manifold between 2.15 ppm and 2.45 ppm [4 hydrogen atoms of the CH_2 groups of the –P–$(CH_2)_2$–P– bridge], a singlet at δ = 2.15 ppm (3 hydrogen atoms of the $NCCH_3$ solvent molecule connected to the metal atom) and a singlet at δ = 1.38 ppm (15 hydrogen atoms of the methyl groups of the Cp* ligand). In addition, the coordination of an $NCCH_3$ molecule on the iron atom is indicated by the presence of a characteristic ν_{CN} band stretch at 2249 cm^{-1} in the IR spectrum. This value is in agreement with those observed in other iron complexes with this same solvent molecule.[24] FT-IR (Nujol): $\tilde{\nu}$ = 2249 (m, $\nu_{C\equiv N}$) cm^{-1}. ^{1}H NMR (200 MHz $CDCl_3$): δ = 7.70–7.34 (m, 20 H, Ph), 2.45–2.45 (m, 4 H, CH_2dppe), 2.15 (s, 3 H, CH_3CN), 1.90 (s, 15 H, Cp*) ppm. ^{31}P NMR (81 MHz, $CDCl_3$): δ = 91.1 (s, dppe) ppm.

Synthesis of $[Cp^*(dppe)Fe–NCMe]_2[Mo_6Br_{14}]$ (2): [Cp*(dppe)FeCl] (0.115 g, 0.36 mmol) and $Cs_2Mo_6Br_{14}$ (0.360 g, 0.18 mmol) were

Table 7. Selected interatomic distances [Å] for [Cp*(dppe)Fe–NCCH$_3$]$_2$[Mo_6I_{14}] (**3**).

Anionic unit: $[Mo_6I^i_8I^a_6]^{2-}$					
Mo–Mo bond lengths					
Mo1–Mo2	2.6765(6)	Mo1–Mo2	2.6802(6)	Mo1–Mo3	2.6801(6)
Mo1–Mo3	2.6844(5)	Mo2–Mo3	2.6745(5)	Mo2–Mo3	2.6878(6)
Mo–I^a bond lengths (^{a}: apical ligand)					
Mo1–I7	2.8427(5)	Mo2–I4	2.8408(5)	Mo3–I6	2.8467(5)
Mo–I^i bond lengths (^{i}: inner ligand)					
Mo1–I1	2.7776(5)	Mo1–I2	2.7736(5)	Mo1–I3	2.7753(5)
Mo1–I5	2.7665(5)	Mo2–I1	2.7745(5)	Mo2–I2	2.7819(5)
Mo2–I3	2.7766(5)	Mo2–I5	2.7808(5)	Mo3–I1	2.7710(5)
Mo3–I2	2.7755(5)	Mo3–I3	2.7788(5)	Mo3–I5	2.7889(5)
Cationic unit: [Cp*(dppe)Fe–NCCH$_3$]$^+$					
Fe–X distances and bond lengths					
X = Cp*					
Fe1–C70	2.127(6)	Fe1–C71	2.121(6)	Fe1–C72	2.108(6)
Fe1–C73	2.118(6)	Fe1–C74	2.135(6)		
X = (dppe)					
Fe1–P1	2.250(2)	Fe1–P2	2.236(2)		
X = NCCH$_3$					
Fe1–N1	1.902(5)				
Cp* intra-bond lengths					
C70–C71	1.44(1)	C71–C72	1.41(1)	C72–C73	1.455(9)
C73–C74	1.414(9)	C74–C70	1.42(1)		
C70–C80	1.53(1)	C71–C81	1.52(1)	C72–C82	1.51(1)
C73–C83	1.48(1)	C74–C84	1.50(1)		
(dppe) intra-bond lengths					
P1–C1	1.843(6)	C1–C2	1.527(9)	C2–P2	1.847(6)
P1–C30	1.850(6)	P1–C40	1.840(6)	P2–C50	1.825(6)
P2–C60	1.826(6)				
C30–C31	1.402(9)	C31–C32	1.40(1)	C32–C33	1.39(1)
C33–C34	1.39(1)	C34–C35	1.40(1)	C35–C30	1.375(9)
C40–C41	1.385(8)	C41–C42	1.39(1)	C42–C43	1.40(1)
C43–C44	1.39(1)	C44–C45	1.40(1)	C45–C40	1.404(9)
C50–C51	1.381(9)	C51–C52	1.39(1)	C52–C53	1.39(1)
C53–C54	1.39(1)	C54–C55	1.38(1)	C55–C50	1.408(9)
C60–C61	1.391(9)	C61–C62	1.40(1)	C62–C63	1.38(1)
C60–C61	1.39(1)	C64–C65	1.40(1)	C65–C60	1.399(8)
–NCCH$_3$ intra-bond lengths					
N1–C3	1.152(8)	C3–C4	1.45(1)		

separately dissolved in degassed MeCN (10 mL and 50 mL, respectively) in Schlenk tubes. The solutions were then mixed together with magnetic stirring. In contrast to [Cp*(dppe)Fe–NCMe]$_2$[$Re_6S_6Br_8$], [Cp*(dppe)Fe–NCMe]$_2$[Mo_6Br_{14}] is not soluble in acetone. Consequently, the solution volume was reduced to 10 mL in order to precipitate all the CsCl which was then separated by filtration. Subsequently, the solvent was removed to provide [Cp*(dppe)Fe–NCMe]$_2$[Mo_6Br_{14}] as an orange crystalline powder (yield 34 %). Suitable single crystals for X-ray diffraction studies were obtained by diffusion of pentane into an acetonitrile solution. EDS analysis did not indicate any traces of Cl or Cs. Heavy-element analyses are in good agreement with the stoichiometry determined from structural data. Spectroscopic characterization (^{31}P NMR, IR) of [Cp*(dppe)Fe–NCMe]$_2$[Mo_6Br_{14}] was carried out and no significant shifts in the band maxima in the IR spectrum or shifts in the NMR peaks could be observed compared with those of [Cp*(dppe)Fe–NCMe]$_2$[$Re_6S_6Br_8$].

Synthesis of [Cp*(dppe)Fe–NCMe]$_2$[Mo_6I_{14}] (3): [Cp*(dppe)Fe–NCMe]$_2$[Mo_6I_{14}] was prepared according to a similar experimental procedure to that described for [Cp*(dppe)Fe–NCMe]$_2$[Mo_6Br_{14}] using Cp*(dppe)FeCl (0.110 g, 0.18 mmol) and $Cs_2Mo_6I_{14}$ (0.230 g, 0.09 mmol). After drying under vacuum, [Cp*(dppe)Fe–NCMe]$_2$[Mo_6I_{14}] was obtained as an orange powder (yield 50 %). Single crystals suitable for X-ray diffraction studies were obtained by diffusion of pentane into an acetonitrile solution. EDS analysss did not suggest any traces of Cl or Cs. Heavy-element analyses are in good agreement with the stoichiometry determined from structural data. Spectroscopic characterization (^{31}P NMR, IR) of [Cp*(dppe)Fe–NCMe]$_2$[Mo_6I_{14}] was carried out and no significant shifts in the band maxima in the IR spectrum or shifts in the NMR peaks could be observed compared with those of [Cp*(dppe)Fe–NCMe]$_2$[$Re_6S_6Br_8$].

Acknowledgments

This work has been supported in part by three research grants from the French Ministry of Research and Education (F. d. M., K. K., G. P.). We would like to thank the Scanning Electron Microscopy Center at the University of Rennes 1 for microanalyses and the Diffraction Center of the University of Rennes 1 for the data collection with the Nonius KappaCCD X-ray diffractometer. In particular, the useful advice of Dr. Thierry Roisnel is gratefully acknowledged. We are also indebted to the French Research Ministry for "ACI Nanosciences 2001 – No. 18-01" contract and to "Fondation Langlois" for financial support.

[1] A. Perrin, M. Sergent, *New J. Chem.* **1988**, *12*, 337.
[2] A. Perricone, A. Slougui, A. Perrin, *Solid State Sci.* **1999**, *1*, 657.
[3] J. P. Gabriel, K. Boubekeur, S. Uriel, P. Batail, *Chem. Rev.* **2001**, *101*, 2037.
[4] A. Perrin, C. Perrin, M. Sergent, *J. Less-Common. Met.* **1988**, *137*, 241.
[5] C. Perrin, *J. Alloys Compd.* **1997**, *262–263*, 10, and references cited therein.
[6] H. Schäfer, H. G. von Schnering, *Angew. Chem.* **1964**, *76*, 833.
[7] R. Chevrel, M. Sergent, "Superconductivity in Ternary Compounds", in *Topics in Current Physics* (Eds.: Ø. Fischer, M. P. Maple), Springer Verlag, Berlin, Heidelberg, New York, **1982**.
[8] *Metal Clusters in Chemistry*, vol. II (Eds.: P. Braunstein, L. A. Oro, P. R. Raithby), Wiley-VCH, Weinheim, **1999**.
[9] J. M. Tarascon, F. J. Di Salvo, D. W. Murphy, G. W. Hull, E. A. Rietman, S. V. Waszczak, *J. Solid State Chem.* **1984**, *54*, 104.
[10] H. D. Selby, B. K. Roland, Z. Zheng, *Acc. Chem. Res.* **2003**, *36*, 933.
[11] M. W. Willer, J. R. Long, C. C. McLauhan, R. Holm, *Inorg. Chem.* **1998**, *37*, 328.
[12] Nonius, *COLLECT, DENZO, SCALEPACK, SORTAV: KappaCCD Program Package*, Nonius B. V., Delft, The Netherlands, **1999**.
[13] J. De Meulenaar, H. Tompa, *Acta Crystallogr., Sect A* **1965**, *19*, 1014.
[14] G. Cascarano, A. Altomare, C. Giacovazzo, A. Guagliardi, A. G. G. Moliterni, D. Siliqi, M. C. Burla, G. Polidori, M. Camalli, *Acta Crystallogr., Sect A* **1996**, *52*, C-79.
[15] D. J. Watkin, C. K. Prout, J. R. Carruthers, P. W. Betteridge, *CRYSTAL*, Chemical Crystallography Laboratory, Oxford, UK, **1999**, issue 11.
[16] A. Slougui, A. Perrin, M. Sergent, *J. Solid State Chem.* **1999**, *147*, 358.

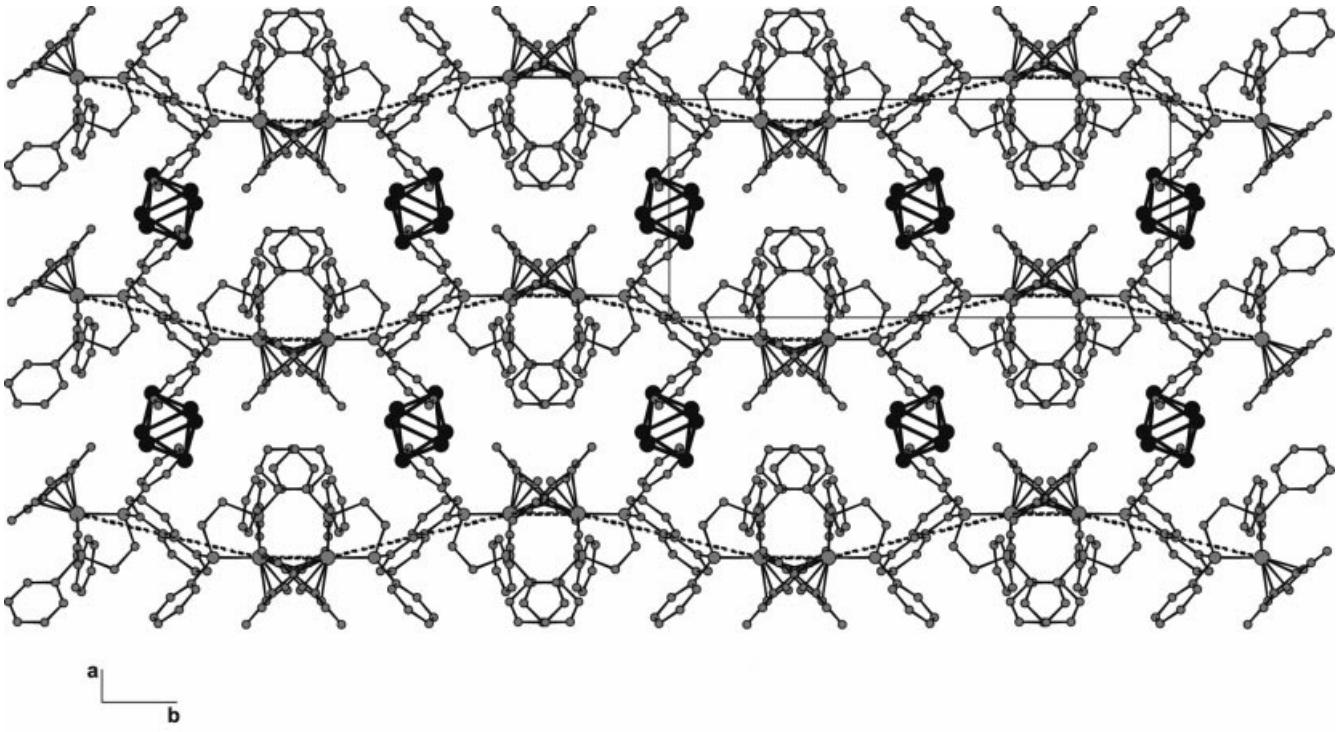

Figure 3. $[Cp^*(dppe)Fe–NCCH_3]_2[Me_6L_{14}]$ (Me = Re, Mo; L = S, Br, I) structure projection in the (*a*,*b*) plane of the unit-cell. Illustration of the anionic/waved cationic layers succession along the *a* axis of the nit-cell.

Table 8. Average bond lengths or interatomic distances [Å] in the structure of the three title compounds, for $[Cp^*(dppe)Fe–NCMe]PF_6$ and for the precursor cesium salts of $[Re_6S_6Br_8]^{2-}$, $[Mo_6Br_{14}]^{2-}$, $[Mo_6I_{14}]^{2-}$ (X = halogen atoms; Y = chalcogen atoms; A = organometallic cation: $[Cp^*(dppe)Fe–NCMe]^+$).

		$A_2[Re_6S_6Br_8]$ (**1**)	$A_2[Mo_6Br_{14}]$ (**2**)	$A_2[Mo_6I_{14}]$ (**3**)	APF_6	$Cs_2[Re_6S_6Br_8]$[22]	$Cs_2[Mo_6Br_{14}]$[23]	$Cs_2[Mo_6I_{14}]$[23]
	M–M	2.605	2.640	2.679		2.592	2.636	2.679
	$M–L^a$	2.537	2.597	2.843		2.520	2.600	2.851
$M–L^i$	$M–X^i$	2.56	2.605	2.777		2.525	2.601	2.779
	$M–Y^i$	2.44	–	–		2.407	–	–
	Fe–C (Cp*)	2.12	2.12	2.12	2.12			
	Fe–N (NCMe)	1.909	1.903	1.902	1.906			
	Fe–P (dppe)	2.24	2.24	2.24	2.23			
	C–C (C_5)	1.43	1.42	1.43	1.42			
Cp*	C–C (C_5–C_5H_{15})	1.51	1.52	1.51	1.51			
	P–C (C_2H_2)	1.86	1.85	1.84	1.84			
(dppe)	C–C (C_2H_2)	1.53	1.52	1.53	1.54			
	P–C (C_6H_6)	1.83	1.83	1.84	1.84			
	C–C (C_6H_6)	1.39	1.39	1.39	1.38			
N≡C–CH_3	N–CCH_3	1.15	1.14	1.15	1.13			
	NC–CH_3	1.46	1.45	1.45	1.45			

[17] J. Ruiz, D. Astruc, J.-P. Bideau, M. Cotrait, *Acta Crystallogr., Sect.C: Cryst. Struct. Commun.* **1990**, *46*, 2367.
[18] F. Paul, C. Lapinte, *Coord. Chem. Rev.* **1998**, *178–180*, 427.
[19] R. Denis, L. Toupet, F. Paul, C. Lapinte, *Organometallics* **2000**, *19*, 4240.
[20] K. Costuas, F. Paul, L. Toupet, J.-F. Halet, C. Lapinte, *Organometallics* **2004**, *23*, 2053.
[21] C. Roger, P. Hamon, L. Toupet, H. Rabaâ, J.-Y. Saillard, J.-R. Hamon, C. Lapinte, *Organometallics* **1991**, *10*, 1045.
[22] G. Pilet, PhD Dissertation, Rennes, France, **2003**.
[23] K. Kirakci, S. Cordier, C. Perrin, *Z. Anorg. Allgem. Chem.*, in press.
[24] D. Catheline, D. Astruc, *Organometallics* **1984**, *3*, 1094.
Received September 24, 2004

